Spin-polarized electron scattering studies of the ferromagnetic glass $Fe_{81.5}B_{14.5}Si_4$

J. Unguris, D. T. Pierce, and R. J. Celotta

National Bureau of Standards, Washington, D.C. 20234

(Received 23 June 1983)

Low-energy [(20—500)-eV] spin-polarized electrons were used to probe the magnetic surface properties of the ferromagnetic metallic glass $Fe_{81.5}B_{14.5}Si_4$. The spin-independent intensity and the spin-dependent asymmetry of the elastic scattering were measured as a function of applied magnetic field, electron energy, scattering angle, and angle of incidence. The scattering is liquidlike with no crystalline diffraction effects. Comparisons are made with scattering from the magnetic glass $Fe_{40}Ni_{40}B_{20}$ and an iron single crystal. Surface hysteresis curves as measured by the spin-dependent elastic scattering are very sensitive to ion-sputtering damage and to subsequent annealing. The asymmetry of the inelastic scattering was also measured for various primary energies and was found to closely resemble the elastic scattering asymmetry.

I. INTRODUCTION

Recently there has been a great deal of interest in using spin-polarized low-energy electron scattering to study magnetic surface properties.[1,2] Among the various electron-spin sensitive techniques in use, polarized low-energy electron diffraction (PLEED) has been shown to be a powerful technique for probing the long-range magnetic order near the surface of a material. A major obstacle in interpreting the results of PLEED experiments, however, is that relatively little is known about the magnetic spin-dependent scattering mechanisms. Attempts at understanding unknown magnetic surface structures through the comparison of PLEED data with model calculations of electron scattering are therefore less conclusive, since the spin-dependent scattering potentials that are required for the calculations are not well known. In an attempt to concentrate on the spin-dependent scattering potentials we have performed a series of experiments in which we have studied the elastic and inelastic scattering of polarized electrons from ferromagnetic metallic glasses. These materials have liquidlike structures that make interpretation of the structural dependence of the electron scattering straightforward. In contrast to crystalline materials which give rise to electron scattering concentrated in sharp diffraction beams, scattering from the magnetic glasses is spread relatively smoothly throughout space and is only weakly dependent upon scattering geometry. The ferromagnetic glasses are thus ideal systems in which to probe and characterize the effective magnetic atomic scattering potentials.

The first measurements of the spin-dependent electron scattering from a ferromagnetic glass were done by Pierce, Celotta, Unguris, and Siegmann on the glass $Fe_{40}Ni_{40}B_{20}$.[3,4] In these works the spin-dependent and spin-independent intensities of elastically and inelastically scattered electrons were measured as a function of energy, scattering angle, and temperature. Pierce et al. showed that, after accounting for the dependence of the electron-beam attenuation with angle of incidence, the spin-independent elastic scattering intensities could be simply attributed to atomic scattering factors and a small uniform background contribution due to multiple scattering. The spin-dependent scattering was also found to be a well-behaved, smooth function of the energy and scattering angle although it does change sign at low energies. Finally, a preliminary measurement of the spin-dependent production of inelastically scattered electrons showed a strong correlation between the elastic and inelastic spin-dependent electron scattering.

Following the work by Pierce et al. on the $Fe_{40}Ni_{40}B_{20}$ glass it was decided to repeat and expand the electron scattering experiments using a different ferromagnetic glass, $Fe_{81.5}B_{14.5}Si_4$. This current work was motivated by several factors. First, this particular glass more nearly approximated the chemical composition of a single-component system and would thus be more useful for making comparisons with PLEED data from Fe single crystals. Second, information about the influence of the Ni in the $Fe_{40}Ni_{40}B_{20}$ glass on the spin-dependent scattering was desired. Third, a more extensive set of elastic scattering measurements was needed for testing various theoretical spin-dependent scattering potentials. And finally, additional information about the dependence of the inelastic scattering on the primary electron energy was needed.

II. APPARATUS

The GaAs-polarized electron source, vacuum chamber, and detection scheme have been described in detail previously.[3,5] For the current work, special low-birefringence windows were added to the vacuum chamber to permit *in situ* measurement of the longitudinal magneto-optic Kerr effect, and the sample holder geometry was changed. In previous experiments the magnetic material under study was placed across the poles of a c-shaped, iron-core magnetizing solenoid. This approach suffered from the fact that the applied magnetic field response of the sample was obscured by the hysteresis curve of the solenoid iron

core. In addition, any small gap between the sample and the iron-core pole pieces resulted in stray magnetic fields, which altered the electron trajectories, and also caused demagnetization fields, which distorted the magnetization hysteresis curve. To solve this problem we use one continuous loop of magnetic glass as the target. The sample consists of a 9.6-mm wide by 0.025-mm thick ribbon of $Fe_{81.5}Ni_{14.5}Si_4$ that is formed into a loop that is 10 cm in circumference. The overlapping ends of the ribbon are mechanically clamped together, and an insulated wire was loosely wrapped around the ribbon to provide the applied magnetic field. Since the easy magnetization axis of the glass, which is determined by anisotropies introduced in casting, is along the length of the ribbon, the loop is very similar to the magnetic picture-frame geometry used in studies of ferromagnetic single crystals.[6]

A schematic of the scattering geometry is shown in Fig. 1. Scattered electrons are detected with a Faraday cup at a scattering angle of θ. The enlarged Faraday cup aperture subtends a full angle of $\Delta\theta = 9°$. The sample normal can be tilted by an angle α with respect to the incident electron beam. The incident electron spin and the sample magnetization direction are both constrained to lie in the scattering plane, so that spin-dependent scattering contributions due to spin-orbit interactions are minimized. The Faraday cup measures the intensity of the scattered electrons when the spin of the incident electrons is parallel to the majority-spin direction in the solid (antiparallel to the magnetization), $I_\uparrow$, and when the incident spins are antiparallel to the majority spins, $I_\downarrow$. The spin dependence of the elastic scattering is then given by the normalized asymmetry which is defined as

$$A \equiv \frac{1}{|P_0\cos\alpha|} \frac{I_\uparrow - I_\downarrow}{I_\uparrow + I_\downarrow} , \qquad (1)$$

where $P_0\cos\alpha$ is the effective component of the polarization of the incident beam. In our particular scattering geometry, A is solely due to exchange scattering and is directly proportional to the magnetization in situations where multiple scattering can be neglected.[2] The spin-independent elastic scattering is given by the spin-averaged intensity $I = (I_\uparrow + I_\downarrow)/2$.

The metallic glass used was made by the chill block melt-spinning technique and hence had a dull surface (melt-block interface) and a shiny surface (melt-air interface). The sample was arranged so that the side of the ribbon that was exposed to air during casting was the surface that was probed by the electron beam. Both sides of the ribbon gave the same satisfactory hysteresis curves when measured by the magneto-optic Kerr effect, but the air side was chosen because of its superior optical quality. The surface was cleaned by sputtering with 500-eV Ar^+ ions followed by annealing to approximately 120 °C. During sample preparation the surface composition was characterized by Auger spectroscopy while the sample magnetic properties were monitored by measuring hysteresis curves with both the Kerr effect and polarized low-energy electron scattering. Figure 2 shows a series of surface hysteresis curves measured during sample preparation. The curves were obtained by measuring the asymmetry of the elastically scattered electrons at 100 eV and $\theta = 166°$ as a function of applied magnetic field. Before sputtering, Auger analysis showed that the surface is oxide covered and no asymmetry is measured. Initial sputtering removes most of the oxide layer and leaves a
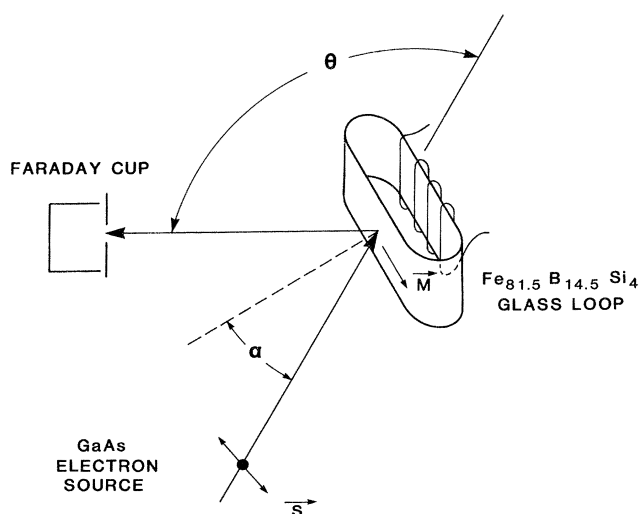

FIG. 1. This scattering geometry schematic shows the relative positions of the electron source, magnetic glass, and Faraday cup. The polarization of the incident electron beam is transverse and lies in the scattering plane as does the sample magnetization.
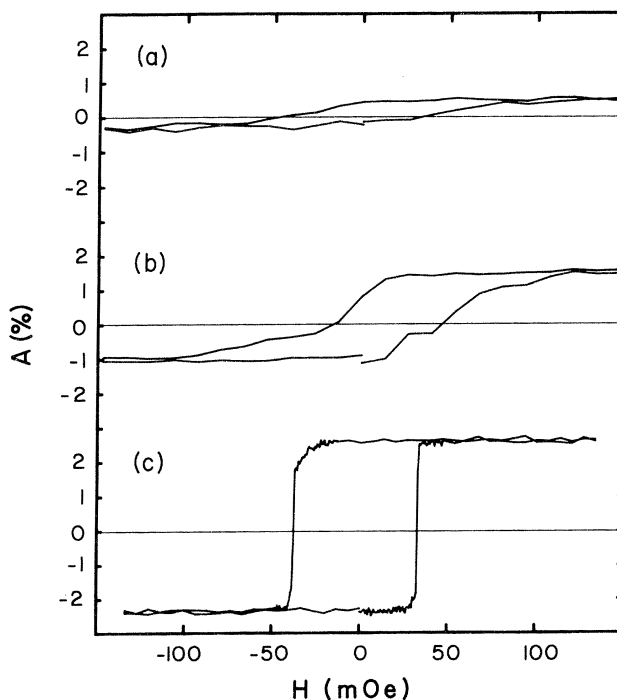

FIG. 2. Surface hysteresis curves measured by the elastic scattering asymmetry are shown as the surface is cleaned: (a) after removal of oxide by sputtering, (b) after prolonged sputtering, and (c) after annealing to 110 °C.

surface consisting primarily of Fe and C but with little B and no Si present. The hysteresis curve for this surface is shown in Fig. 2(a). Following a more prolonged ion bombardment, after which about 500 Å of material had been removed, the improved hysteresis curve in Fig. 2(b) appears. Auger analysis of this surface revealed the following composition: C, 11 at. %; Fe, 79 at. %; B, 8 at. %; Si, 2 at. % (assuming a homogeneous surface composition). Thus although there is still a significant amount of C present, the relative amounts of Fe, B, and Si present approximately the bulk concentrations. Further sputtering does not significantly change the surface composition or the shape of the hysteresis curve, but annealing to 120 °C for 1 min produces the square hysteresis curve shown in Fig. 2(c) without altering the surface composition.

The increase in hysteresis loop squareness and the reduction in coercive force that occur after annealing are presumably the result of removing ion-bombardment—induced strains in the surface of the material. Such strains create magnetic anisotropies in the surface because of strain-magnetostriction interactions, and thus degrade the hysteresis loop quality. Similar relaxation effects are observed in bulk magnetic properties only at higher temperatures. For bulk $Fe_{81.5}B_{14.5}Si_4$ the crystallization temperature is about 450 °C, and annealing occurs at approximately 200 °C.[7,8]

Hysteresis curves were also measured during sample preparation using the magneto-optic Kerr effect. These measurements produced square hysteresis curves, similar in shape to one shown in Fig. 2(c) and with the same value of the coercive field. The optically measured hysteresis curves did not change during the surface preparation. Since the optical measurement probes to a depth of approximately 150 Å it is essentially a bulk magnetization measurement when compared to the electron scattering with its sampling depth of about 3 Å at an electron energy of 100 eV. Thus our surface preparation procedures do not alter the bulk magnetic properties.

III. RESULTS

Measurements of the elastically scattered asymmetry $A(E)$ and intensity $I(E)$ as a function of energy are shown in Fig. 3 for various scattering angles. The measurements were made at normal incidence and using an annealed magnetic glass after it had been driven to saturation and then had the applied field turned down to zero. The data are very similar to those obtained by Pierce et al. for $Fe_{40}Ni_{40}B_{20}$.[1] As in the case of $Fe_{40}Ni_{40}B_{20}$, the scattered intensities are atomiclike and are essentially independent of angle of incidence after attenuation of the electron beam in the solid has been accounted for.[3] The asymmetries are characterized by two changes in sign at low energies that shift slightly with scattering angle. In addition, for $\theta = 166°$ the asymmetry was measured up to an energy of 800 eV. For energies greater than 200 eV, $A(E)$ decreased asymptotically to zero, and no additional structures associated with asymmetry changes greater than $\Delta A(E) = 0.003$ were observed. Extrinsic apparatus-related asymmetries were checked for by repeating several of the $A(E)$ measurements with the sample magnetization re-
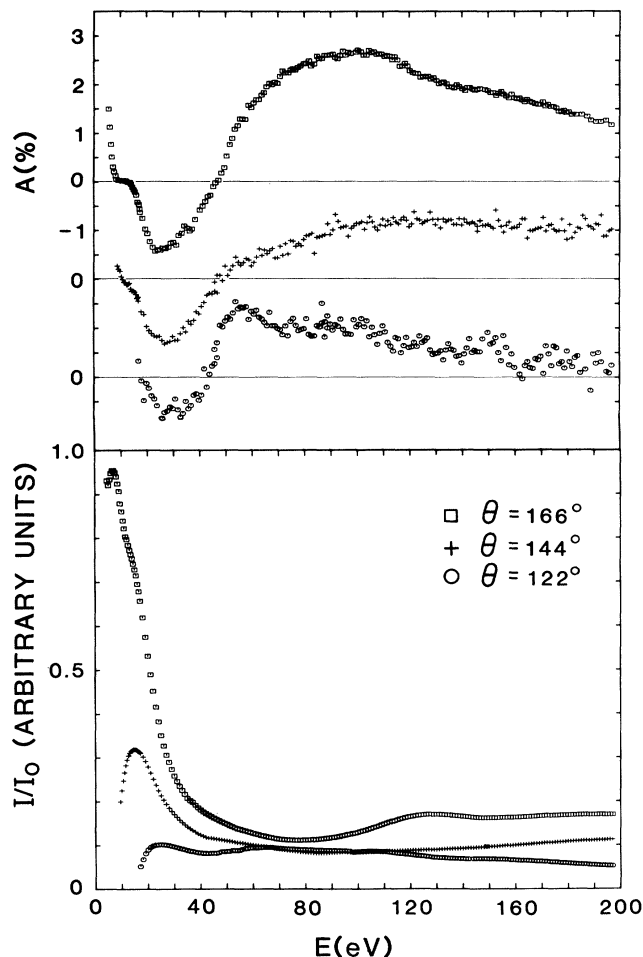

FIG. 3. Elastic scattering asymmetry $A(E)$ and intensity $I(E)/I_0$ are shown as a function of energy for different scattering angles. (I_0 is the incident current.)

versed. No extrinsic asymmetry could be detected.

It should also be noted that while the data presented in Fig. 3 are for clean annealed samples, measurements were also made on surfaces that were somewhat more contaminated or less well annealed. The effect of these surface imperfections is to attenuate uniformly the magnitude of the $A(E)$ measured, but the energy and angle dependence of $A(E)$ is unchanged.

Among the various theoretical models that have been applied to describe the spin-dependent scattering from a magnetic surface, the simplest approach has been to treat the scattering in the first Born approximation.[9] To test this approach the asymmetry data in Fig. 3 have been plotted as a function of the momentum transfer of the scattered electrons and are displayed in Fig. 4. Although there are qualitative similarities between the data, there are also significant differences between the measurements at various scattering angles. A Born-approximation treatment of the scattering should thus at best provide a qualitative description of the spin-dependent electron scattering and should be used with caution when attempting to relate the scattering to magnetic structures.
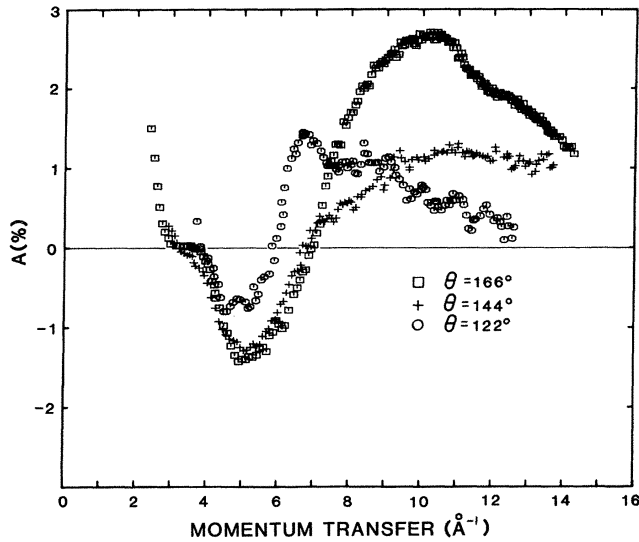
FIG. 4. Asymmetry data of Fig. 3 are shown plotted as a function of momentum transfer.

In order to examine the influence of compositional and structural changes upon asymmetry and intensity measurements, the measured energy dependence of $A(E)$ and $I(E)$ are shown in Fig. 5 for the $Fe_{81.5}B_{14.5}Si_4$ and $Fe_{40}Ni_{40}B_{20}$ magnetic glasses and for the (100) surface of an Fe single crystal. Both sets of glass data are measured at $\theta = 166°$. The Fe(100) crystal data are the result of our
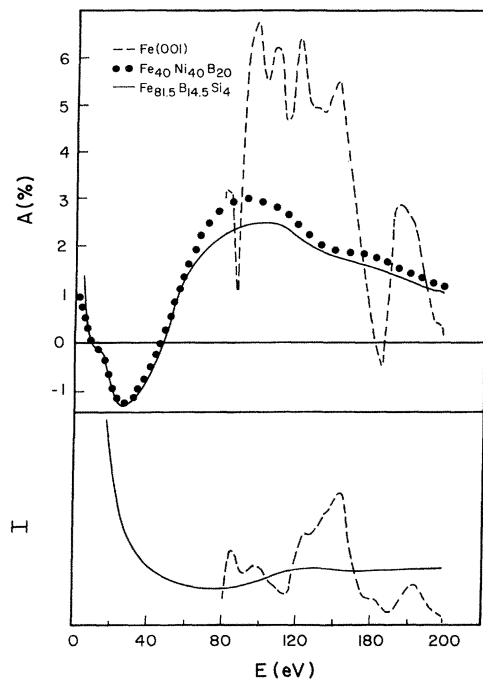

FIG. 5. Elastic scattering asymmetries measured for the ferromagnetic glasses $Fe_{81.5}B_{14.5}Si_4$ and $Fe_{40}Ni_{40}B_{20}$ and for an Fe(100) crystal are compared. Measurements were made for $\theta = 166°$ and the (00) beam for the crystal. Also shown are the Fe glass and Fe crystal intensity curves.

preliminary measurements and are for the (00) diffraction beam at an angle of incidence of 7°, corresponding to a scattering angle of 166°. The differences between the Fe glass and the Fe crystal measurements are obvious and large. The periodic lattice of the crystal results in the complicated, somewhat periodic, diffraction structure in the scattered intensity. The influence of the crystal structure factor can also be observed in the asymmetry measurement, which is much more complicated than that for the glass. In contrast the data for the two different ferromagnetic glasses are almost identical. The only difference is a slightly enhanced peak in the $Fe_{40}Ni_{40}B_{20}$ glass asymmetry near 100 eV. The similarity between $A(E)$ curves for the glasses is consistent with bulk magnetization measurements which show that while each Fe atom contributes 2.1 Bohr magnetons to the glass magnetization, each Ni atom only adds 0.6 Bohr magnetons.[10] The Ni atoms contribute relatively weakly, therefore, to the spin-dependent scattering. In addition, since the Ni and Fe atomic scattering cross sections are very similar, the Ni contribution to the spin-independent intensity will be about the same as that from Fe.[11] Thus the general shape of the measured asymmetry is dominated by the scattering from Fe, which is consistent with our observations.

One feature of the data that is somewhat puzzling is the similarity in magnitude of the Fe and FeNi glass asymmetries. $Fe_{81.5}B_{14.5}Si_4$ with a magnetic moment of 1.5 Bohr magnetons per atom alloy should yield a larger asymmetry than $Fe_{40}Ni_{40}B_{20}$, which has 1.1 Bohr magnetons per atom alloy. Since the Fe and Ni atomic scattering factors are about equal and both glasses have equal amounts of metalloid and carbon contamination present, we would expect that the Fe glass asymmetry should be almost 50% larger than the FeNi glass asymmetry. Differences between the bulk and the Auger measured surface stoichiometries can only account for 10% changes in the saturation magnetization if bulk phase diagrams are valid at the surface.[7] One possibility for the reduced Fe glass asymmetry is that the surface is not as well ordered magnetically as the FeNi glass. A higher degree of residual disorder in the surface could reduce the magnetization and thus the asymmetry. This is consistent with the greater sensitivity of the Fe glass to ion-sputtering damage and annealing. This surface disorder might also explain why the Fe glass $A(E)$ is less than the energy-averaged $A(E)$ of the Fe crystal.

As a check on the importance of diffraction and multiple scattering effects, asymmetry measurements were made at various angles of incidence. Figure 6 shows the results of asymmetry measurements as a function of scattering angle for various electron energies and angles of incidence. As can be seen from the data, the asymmetry is relatively insensitive to changes in the angle of incidence. Crystalline diffraction and multiple scattering effects are thus not important, and the scattering is essentially liquid-like.

In addition to studies of the elastically scattered electron asymmetry, measurements were also made of the asymmetry of electrons that had suffered energy losses in the magnetic glass. The first measurements of the spin-dependent asymmetry of inelastic scattering were done by
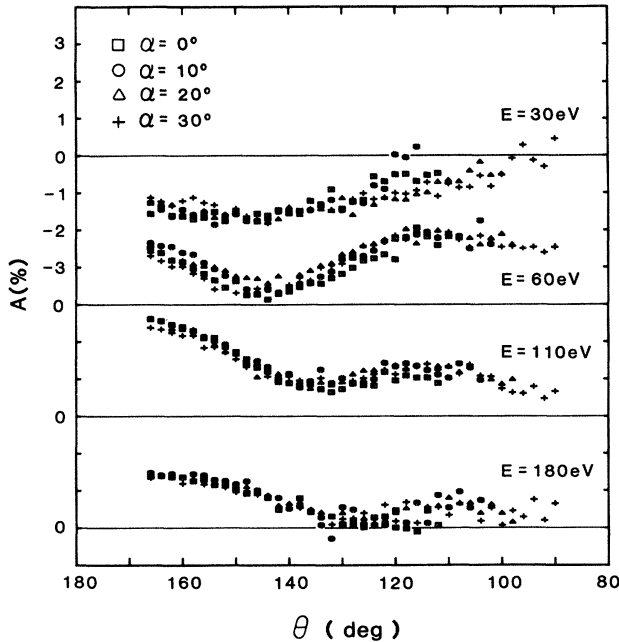
FIG. 6. Elastic scattering asymmetry is shown as a function of scattering angle for various energies and angles of incidence.

Siegmann et al. for the magnetic glass $Fe_{40}Ni_{40}B_{20}$.[4] This work, which primarily focused on understanding the spin dependence of the current absorbed by a ferromagnetic metal, found significant correlations between the elastic and inelastic electron asymmetries. Because such information might be useful in understanding the interplay between elastic and inelastic scattering processes in the solid, similar measurements were also made for the $Fe_{81.5}B_{14.5}Si_4$ glass. The measurements were made by using the Faraday-cup suppressor lens as a retarding field energy analyzer. With a fixed energy beam incident on the sample, the current to the Faraday cup was measured as a function of the retarding voltage applied to the suppressor. This integrated current was then differentiated numerically, and we thus obtained the number of electrons $N(E)$ backscattered from the sample to the Faraday cup as a function of energy E for some primary beam energy E_p. Measurements were made for incident electron spins parallel to the majority spins $N_\uparrow(E)$ and for incident spins antiparallel to majority spins $N_\downarrow(E)$. The asymmetry of the production of inelastically scattered electrons is then defined as

$$A(N(E)) \equiv \frac{1}{|P_0 \cos\alpha|} \frac{N_\uparrow(E) - N_\downarrow(E)}{N_\uparrow(E) + N_\downarrow(E)} .$$

Figure 7 shows $A(N(E))$ measured at a scattering angle of 166° for primary energies of 54, 110, and 180 eV. For comparison, the elastic scattering asymmetry at $\theta = 166°$ is also shown. Just as for the $Fe_{40}Ni_{40}B_{20}$ glass data, $A(N(E))$ is qualitatively similar to $A(E)$. Both $A(N(E))$ and $A(E)$ have about the same sign and magnitude, although the sign change in $A(N(E))$ that corresponds to the 50-eV sign change that occurs in $A(E)$ moves to higher energies with increasing primary energy. In addition, as in the case of the FeNi glass, $A(N(E))$ goes to

zero at very low energies where the majority of electrons produced are true secondaries. The true secondary-electron production thus does not depend upon the spin of the incident electrons. One should note, however, that these low-energy secondary electrons, especially those emitted near 0 eV, are polarized. Several experiments have shown that these secondaries in the (0—10)-eV energy range have polarizations that are as large or larger than the polarization of the bulk electronic valence bands.[12—14]

The strong similarity between the elastic and inelastic scattering asymmetries suggests that the elastic scattering plays a major role in determining $A(N(E))$. In fact, with the additional spin-dependent information about the inelastic scattering one can potentially differentiate between various secondary-electron production mechanisms that depend in different ways upon the spin of the incident electron. This spin sensitivity can provide new information about the relative importance of elastic and inelastic scattering processes in secondary-electron emission. As a first step in this direction, we have attempted to model the secondary-electron production as a simple two-step process which consists of an inelastic event with small momentum transfer and an elastic, large angle, backscattering which redirects the electron toward the surface. Similar two-step models have been used to differentiate between inelastic and elastic processes in electron energy-loss spectra from crystalline solids.[15] In applying this two-step model we are excluding those electrons that have been multiply elastically scattered or have suffered large ($\Delta E > E_p/2$) energy losses. Thus the model should work best for rediffused primaries with energies $E_p/2 < E < E_p$ and worst for the true secondaries with $E \lesssim 20$ eV. Spin-
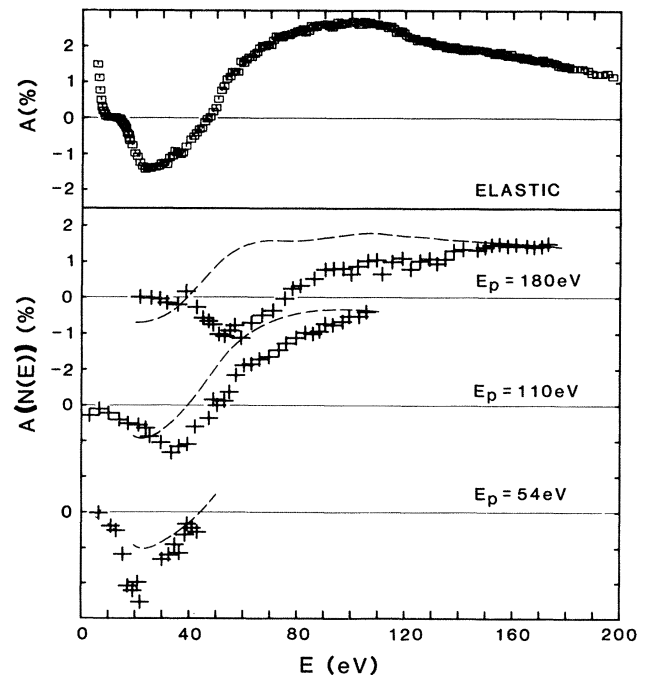

FIG. 7. Measured and calculated (dashed lines) asymmetry of the inelastic electron scattering $A(N(E))$ is shown as a function of energy for various primary energies. The elastic asymmetry is also shown for comparison. All of the data are for $\theta = 166°$.

dependent effects in the electron mean free paths[16,17] and the production of secondary electrons,[13] which are important for lower-energy electrons, are not included in this model. The final assumption is that the energy loss only involves excitations that do not depend significantly upon the spin of the incident electron.

Following these assumptions we can predict two different possible $A(N(E))$ curves depending upon whether the inelastic event precedes the elastic or vice versa. If the electron is elastically scattered first and then loses energy, $A(N(E))$ would equal $A(E_p)$ and be independent of E. On the other hand, if the elastic scattering occurs last then $A(N(E))$ should be approximately equal to $A(E)$. In this case, how closely $A(N(E))$ actually resembles $A(E)$ is determined by how much the inelastic scattering changes the direction of the primary electron, but for small angular deviations ($\sim \pm 10°$) one can see from Fig. 6 that these corrections would be small. As a first approximation one might assume that either scattering sequence is equally probable, except that the relative strengths of the two processes are determined by the energy dependence of the spin-independent elastic scattering cross sections. The inelastic asymmetry for a single-component system with no multiple scattering can then be written as

$$A(N(E)) = \frac{|f(E_p)|^2 A(E_p) + |f(E)|^2 A(E)}{|f(E_p)|^2 + |f(E)|^2} \, ,$$

where $|f(E)|$ is the magnitude of the spin-independent atomic scattering factor. Using calculated atomic scattering cross sections[11] for Fe and assuming no angular deflection by the inelastic scattering, we obtain the inelastic asymmetries shown in Fig. 7. Since $|f(E)|^2$ for this scattering angle has a minimum at about 90 eV and becomes very large at lower energies, the calculated $A(N(E))$ is dominated at low energies by electrons that were scattered inelastically first. For energies above 90 eV, elastic scattering before energy loss is favored. This model is in qualitative agreement with what is observed for 54- and 110-eV primary energies. For 180 eV the agreement is not as good. Perhaps some of the discrepancy could be resolved if the spin and scattering angle

dependence of the inelastic scattering and of the elastic multiple scattering were better known and could be included in the model.

IV. CONCLUSION

Spin-polarized electron scattering from ferromagnetic glasses offers new information about the fundamental interactions of electrons with magnetic materials and about the magnetic surface properties of the glasses themselves. In this work we have accumulated a large amount of spin-dependent elastic scattering data for low-energy electrons scattered from a primarily single-component Fe glass. Since the elastic scattering is free from crystalline diffraction effects and thus is essentially atomiclike, these asymmetry data provide a possible test of different models for the effective magnetic atomic scattering potentials. The scattering potentials should be able to explain the glass data before being used to analyze the more complicated structural information available in scattering from magnetic crystals. We have also demonstrated how the addition of spin-dependent information about the inelastic scattering can be used to differentiate between the various elastic and inelastic mechanisms involved. An appealing feature of using magnetic glasses is the wide variety of elements and compositions that is available. Thus systematic studies of the dependence of the spin-dependent electron scattering upon surface composition, such as our comparisons of the Fe glass and the FeNi glass data, should be more tractable than with single crystals; although it is more difficult to prepare clean surfaces with the glasses. And finally we have shown that the spin-polarized scattering is a useful tool for monitoring the surface magnetization during ion bombardment and heat treatment of the ferromagnetic metallic glass.

ACKNOWLEDGMENTS

[1]D. T. Pierce and R. J. Celotta, Adv. Electron. Electron. Phys. 56, 219 (1981).

[2]R. Feder, J. Phys. C 14, 2049 (1981).

[3]D. T. Pierce, R. J. Celotta, J. Unguris, and H. C. Siegmann, Phys. Rev B 26, 2566 (1982).

[4]H. C. Siegmann, D. T. Pierce, and R. J. Celotta, Phys. Rev. Lett. 46, 452 (1981).

[5]D. T. Pierce, R. J. Celotta, G.-C. Wang, W. N. Unertl, A. Galejs, C. E. Kuyatt, and S. R. Mielczarek, Rev. Sci. Instrum. 51, 478 (1980).

[6]See, for example, S. F. Alvarado, M. Campagna, and H. Hopster, Phys. Rev. Lett. 48, 51 (1982).

[7]F. E. Luborsky, J. J. Becker, J. L. Walter, and H. H. Liebermann, IEEE Trans. Magn. MAG-15, 1146 (1979).

[8]F. E. Luborsky, in Ferromagnetic Materials, edited by E. P. Wohlfarth (North-Holland, Amsterdam, 1980), Vol. 1, p. 451.

[9]See, for example, X. I. Saldana and J. Helman, Phys. Rev. B 16, 4978 (1977).

[10]J. J. Becker, F. E. Luborsky, and J. L. Walter, IEEE Trans. Magn. MAG-13, 988 (1977).

[11]M. Fink, M. R. Martin, and G. Somorjai, Surf. Sci. 29, 303 (1972).

[12]J. Unguris, D. T. Pierce, A. Galejs, and R. J. Celotta, Phys. Rev. Lett. 49, 72 (1982).

[13]H. Hopster, R. Raue, E. Kisker, G. Guntherodt, and M. Campagna, Phys. Rev. Lett. 50, 70 (1983).

[14]E. Kisker, W. Gudat, and K. Schroder, Solid State Commun. 44, 561 (1982).

[15]E. Sickafus and F. Steinrisser, Phys. Rev. B 6, 3714 (1972).

[16]R. W. Rendell and D. R. Penn, Phys. Rev. Lett. 45, 2057 (1980).

[17]J. A. D. Matthew, Phys. Rev. B 25, 3326 (1982).